Clinical, functional and genetic characterization of Sixteen Patients Suffering from Chronic Granulomatous Disease variants - Identification of Twelve Novel Mutations in *CYBB*

Michelle Mollin[µ], Sylvain Beaumel[µ], Bénédicte Vigne[µ], Julie Brault[µ], Nathalie Roux-Buisson[µ,£], John Rendu[µ,£], Vincent Barlogis[¤], Gaud Catho[#], Claire Dumeril[%], Fanny Fouyssac[@], Delphine Monnier[¨], Virginie Gandemer[£], Matthieu Revest[+], Jean-Paul Brion[^], Cécile Bost-Bru[&], Eric Jeziorski[~], Laurence Eitenschenck[%], Clémence Jarrasse[%], Stéphanie Drillon Haus[}], Marie Houachée-Chardin[#], Morgane Hancart[~], Gérard Michel[¤], Yves Bertrand[#], Dominique Plantaz[&], Jadranka Kelecic[°], Rasa Traberg[ſ], Leena Kainulainen[=,*], Julien Fauré[µ,£], Franck Fieschi[§], Marie José Stasia[µ,§]

[µ]Centre Hospitalier Universitaire Grenoble Alpes, Pôle de Biologie, CGD Diagnosis and Research Centre (CDiReC), Grenoble, France

[µ]Centre Hospitalier Universitaire Grenoble Alpes, Pôle de Biologie, Laboratoire de Biochimie et Génétique Moléculaire and [£]Univ. Grenoble Alpes, Inserm U1216, Grenoble Institut Neurosciences, Grenoble, France

[¤]Centre Hospitalier Universitaire La Timone, Service de Pédiatrie et Hématologie Pédiatrique, Marseille, France

[#]Hospices Civiles de Lyon, Institut d'Hématologie et d'Oncologie Pédiatrique, Lyon, France

[%]Centre Hospitalier Annecy Genevois, Service de Pédiatrie, Pringy, France

[@]Centre Hospitalier Universitaire de Nancy, Département d'Onco-hématologie Pédiatrique, Vandoeuvre-lès-Nancy, France

[¨]Centre Hospitalier Universitaire Pontchaillou, Laboratoire d'Immunologie cellulaire, Rennes, France

[£]Centre Hospitalier Universitaire de Rennes, Service d'Onco-hématologie Pédiatrique, Rennes, France

[+]Centre Hospitalier Universitaire de Rennes, Service des Maladies Infectieuses et Réanimation Médicale, Rennes, France

[^]Centre Hospitalier Universitaire Grenoble Alpes, Pôle Médecine Aigue et Communautaire, Service d'Infectiologie, Grenoble, France

[&]Centre Hospitalier Universitaire Grenoble Alpes, Département de Pédiatrie, Grenoble, France

[~]Département urgences post-urgences, CHU Montpellier, Pathogenesis and Control of Chronic Infections, INSERM, Université de Montpellier, Montpellier, France

[}]Centre Hospitalier Universitaire de Strasbourg, Hôpital de Hautepierre, Service de Pédiatrie et Onco-hématologie, Strasbourg, France

[°]Klinicki Bolnicki Centar Zagreb, Zagreb, Croatia

[ſ]Hospital of Lithuanian University of Health Sciences, Kauno klinikos, Kaunas, Lithuania

[=]University Hospital of Turku, Department of Pediatrics, Finland and [*]University of Turku, Faculty of Medicine Turku, Finland

[§]Univ. Grenoble Alpes, CEA, CNRS, IBS, F-38044 Grenoble, France

Short tittle: Clinical, functional and molecular characterization of X-linked CGD variant cases

Keywords: X-linked CGD variants; NADPH oxidase; NOX; clinical severity

Correspondence: Marie Jose Stasia; Centre Hospitalier Universitaire Grenoble Alpes, Pôle de Biologie, CGD Diagnosis and Research Centre (CDiReC), Grenoble, France. E-mail: marie-jose.stasia@univ-grenoble-alpes.fr; ORCID number 0000-0003-4466-4880

Abstract

Chronic Granulomatous Disease (CGD) is a rare inherited disorder in which phagocytes lack NADPH oxidase activity. The most common form is the X-linked CGD (X-CGD), caused by mutations in the *CYBB* gene. Clinical, functional and genetic characterizations of 16 CGD cases of male patients and their relatives were done. We classified them as suffering from different variants of CGD ($X91^0$, $X91^-$ or $X91^+$) according to NOX2 expression and NADPH oxidase activity in neutrophils. Twelve mutations were novel (10 $X91^0$-CGD and 2 $X91^-$-CGD). One $X91^0$-CGD was due to a new and extremely rare double missense mutation Thr208Arg-Thr503Ile. We investigated the pathological impact of each single using stable transfection of each mutated cDNA in the NOX2 knock-out PLB-985 cell line. Both mutations leading to $X91^-$-CGD were also novel; one deletion -67delT was localized in the promoter region of *CYBB*, the second one c.253-1879A>G mutation activates a splicing donor site, which unveils a cryptic acceptor site, leading to the inclusion of a 124-nucleotide pseudo-exon between exons 3 and 4 and responsible for the partial loss of NOX2 expression. Both $X91^-$-CGD mutations were characterized by a low cytochrome b_{558} expression and a faint NADPH oxidase activity. The functional impact of new missense mutations is discussed in the context of a new 3D-model of the dehydrogenase domain of NOX2. Our study demonstrates that low NADPH oxidase activity found in both $X91^-$-CGD patients correlates with mild clinical forms of CGD whereas $X91^0$-CGD and $X91^+$-CGD cases remain the most clinically severe forms.

Introduction

Chronic granulomatous disease (CGD) is a rare genetic disorder belonging to innate immunodeficiency syndromes [1]. CGD is due to a defect in the NADPH oxidase complex of phagocytes, highly expressed in phagocytic cells like neutrophils, monocytes and macrophages. The pathophysiological consequence is a defect in reactive oxygen species (ROS) production normally responsible for the killing of bacteria and fungi during an infection. Thus, CGD is generally diagnosed early, before the age of 2 by recurrent and severe infections, although some rare cases may remain undiagnosed until later childhood or even adult life [2]. The incidence of CGD is about 1 in 250,000 newborn individuals. CGD is a genetically heterogeneous disease with all ethnic groups equally affected. The NADPH oxidase complex is composed of a membrane-bound flavocytochrome b_{558} (cytb_{558}), the redox center of the enzyme, consisting of an α subunit, $p22^{phox}$, and a β subunit, NOX2 (also named $gp91^{phox}$), and three cytosolic components: $p47^{phox}$, $p67^{phox}$ and $p40^{phox}$. CGD is caused by mutations located in any of these five subunits [3, 4, 5]. NOX2 is the flavin- and heme-containing oxidase element capable of transferring electrons from NADPH in the cytosol to molecular oxygen in the extracellular or intra-phagosomal compartment, while $p22^{phox}$ stabilizes the expression of this component in phagocytic cells [6]. In neutrophils, the defect in expression of one of these two subunits compromises the expression of the other [7]. Recently it was demonstrated that mutations in EROS/CYBC1 are responsible for a decrease in NADPH oxidase activity of phagocytes lead to chronic granulomatous disease [8]. A small G protein, Rac2 is also involved in regulating NADPH oxidase activity and can be mutated in rare cases, leading to an innate immunodeficiency [9-15]. In resting cells, membrane and cytosolic components of the NADPH oxidase complex are dissociated, while in stimulated phagocytes they become associated at the membrane, leading to an active oxidase complex able to produce superoxide anions [16].

On the basis of the mode of inheritance, two classical forms of the CGD are known: an autosomal form (AR-CGD) with mutations in *CYBA* (OMIM number 233690), *NCF1* (OMIM number 233700), *NCF2* (OMIM number 233710) or *NCF4* (OMIM number 613960), encoding $p22^{phox}$, $p47^{phox}$, $p67^{phox}$ and $p40^{phox}$ proteins, respectively. In the X-linked form of CGD (X91-CGD), mutations are present in *CYBB* (OMIM number 306400) encoding NOX2, which accounts for more than 60% of all CGD cases. Clear information on the severity of CGD according to the genetic forms is often difficult to establish. However, the majority of mutations affecting the membrane cytb_{558} are mainly associated with severe clinical features of CGD, when no measurable NADPH oxidase activity is found [17, 18]. Indeed, X-CGDpatients with mutations in *CYBB* can be classified as having different variant forms ($X91^0$, $X91^-$ or $X91^+$), according to the level of cytb_{558} expression and NADPH oxidase activity in their phagocytes [19]. The *CYBB* gene, encoding NOX2, encompasses 13 exons spanning about 30 kb of the human X chromosome DNA [20, 21]. $X91^0$-CGD, which represents more than 90% of X-CGDcases, is characterized by an absence of cytb_{558} expression and NADPH oxidase activity and is related to the most severe clinical form. A few numbers of cases with "variant" forms of the disease, called $X91^-$-CGD have also been described, in which low levels of cytb_{558} expression can be accompanied by a proportionally decreased NADPH oxidase activity [22]. Mutations associated with this phenotype are usually located in the coding region of *CYBB*. These variants are of interest because they cause a structural disorganization, leading either to an incomplete loss of protein or to a partial dysfunction, or both [23]. The severity of the clinical forms of these variants varies considerably, relating to the level of NADPH oxidase activity [24]. Very rare mutations (5 published cases) in the upstream promoter region of *CYBB*, leading to the $X91^-$-CGD phenotype have also been described [25, 26 , 27, 28]. These mutations are located between the "CCAAT" and the "TATA" boxes in a consensus binding site for the ets family of transcription factors in the NOX2 promoter region, and are responsible for defects in *CYBB* transcription [29]. A striking point is that in most of the $X91^-$-CGD cases characterized by a mutation in the *CYBB* promoter, the CGD diagnosis is made in adolescents (<10 years) or in adults, and usually the clinical form is mild. In the last rare cases of variants, named $X91^+$-CGD, mutated NOX2 is normally expressed (and membrane cytb_{558} too), but no NADPH oxidase activity can be detected. To date about 25 $X91^+$-CGD mutations have been reported [4]. Most of them are missense mutations or small deletions, and are primarily located in the C-terminal cytosolic tail of NOX2, confirming the importance of this region in catalytic activity, but not in structural stability. This feature can be used to obtain insight in the importance of certain regions, but due to the scarcity of patient material, model systems are usually employed for detailed studies. Indeed 18 $X91^+$-CGD mutations have been reproduced in the PLB-985 cell line by mutagenesis, stable transfection and clonal selection, for functional studies [30-36].

We investigated 16 male patients suspected of suffering from X-linked CGD and their families. Clinical, genotypic, and phenotypic data are reported. These X-CGD patients were classified as having different variant forms of CGD ($X91^0$, $X91^-$ or $X91^+$) according to their NOX2 expression and NADPH oxidase activity. Twelve mutations in *CYBB* were novel. Two rare novel mutations (-67delT and a c.253-1879A>G mutation activating a splicing donor site) leading to $X91^-$-CGD were fully characterized. The impact of an intriguing double missense mutation Thr208Arg-Thr503Ile was also deciphered after stable transfection of Thr208Arg-NOX2 and Thr503Ile-NOX2 in the NOX2 knock-out PLB-985 cell line. The functional importance of novel missense mutations is discussed in the context of a new 3D model of dehydrogenase domain of NOX2 [37].

Materials and Methods

Ethical considerations

Blood samples were collected from healthy volunteers, patients and relatives after obtaining their signed informed consent. Written consent for DNA analysis of samples from patients, parents and relatives was also obtained.

Patients

Patients from France, Croatia, Lithuania, and Finland were diagnosed as having CGD on the basis of their clinical history, examination and the inability of their phagocytes to generate reactive oxygen species (Tables 1 and 2). The results of the mosaic pattern by nitroblue-tetrazolium (NBT) assay or dihydrorhodamine-1, 2, 3 (DHR) flow cytometry from the mothers' peripheral neutrophils were consistent with an X-linked inheritance of the disease of their sons. X-CGD subtypes were determined according to the nomenclature $X91^{0}$, $X91^{-}$, $X91^{+}$ where the superscript denotes whether the level of NOX2 is undetectable (0), low (−) or normal (+) as determined by immunoblot or flow cytometry analysis. A summary of the clinical history of the patients is given in Table I. All patients are currently in good health under prophylactic treatment and are under constant care and follow-up in a specialized medical center.

Cell preparation

Human neutrophils and mononuclear cells (lymphocytes plus monocytes) were isolated from citrated blood from patients, their relatives, and healthy volunteers. Lymphocytes purified by Ficoll-Hypaque density gradient centrifugation were infected with the B95-8 strain of EBV and cultured, as previously described [38, 39].

Wild-type (WT), X-CGD (lacking NOX2 expression and/or NADPH oxidase activity) and transfected X-CGD PLB-985 cell lines were grown in RPMI-1640 supplemented with 10% (v/v) fetal bovine serum, 100 units/ml penicillin, 100 µg/ml streptomycin, 2 mM L-Glutamine at 37 °C in a humidified 5% CO_2 atmosphere. Geneticin (0.5 mg/mL) was added to maintain the selection pressure of the plasmid in the transfected cells. For granulocytic differentiation, PLB-985 cells were exposed to 0.5% (v/v) dimethylformamide for 6 days [40].

ROS measurements in phagocytic cells

Reactive oxygen species (ROS) production in human neutrophils was measured by SOD-sensitive cytochrome *c* reduction, resorufine fluorescence measurement (Amplex Red® hydrogen peroxide/peroxidase assay kit, Invitrogen Life technologies, Villebon sur Yvette, France), flow cytometry with dihydrorodamine-1,2,3 (DHR) (TebuBio, Le Perray-en-Yvelines, France) or NBT slide test after opsonized latex bead phagocytosis, as previously described [41]. In flow cytometry experiments with DHR, 5 µg/mL of catalase were added to the mother's neutrophils to avoid passive diffusion of ROS from oxidase-positive cells to oxidase-negative cells. ROS production in PLB-985 cell lines was measured by chemiluminescence in the presence of luminol and horseradish peroxidase (HRPO) [33]. Relative light units (RLU) were recorded at 37°C, over a time course of 60 min in a Luminoscan luminometer (Labsystems, Helsinki, Finland). In some experiment cells were labelled with 2.5 µg/mL Alexa Fluor 647 rat anti-human CD294 (CRTH2, BD Biosciences) as described below, prior of the incubation with DHR and PMA stimulation [28].

NADPH oxidase sub-units and CD294 expression in phagocytic cells

Flow cytometry – Single staining

Monoclonal antibody (mab) 7D5 directed against external epitopes of NOX2 (D162-3, Clinisciences, Nanterre, France), monoclonal anti-p22^{phox} (SC-130550, Santa Cruz Biotechnologies Inc, Heidelberg, Germany), with secondary antibody conjugated with Alexa Fluor 488 (A11070, Invitrogen Life technologies, Villebon sur Yvette, France) or PE (A10543, Invitrogen Life technologies, Villebon sur Yvette, France), were used for analysis of NADPH oxidase subunits expression in phagocytic cells. Control staining with appropriate isotype-matched control antibodies was included to establish thresholds for positive staining. Cell fluorescence was quantified using a FACS Canto II (BD Biosciences). Data were collected and analysed with the FACS DIVA software and FlowJo software-Tree Star (BD Biosciences, Pont de Claix, France).

Expression of NOX2 and CD294 in neutrophils and eosinophils by flow cytometry

Granulocytes (10^6 cells) were suspended in 0.1 mL of HBS-BSA and incubated with 5 µg/mL of mab 7D5 (anti-gp91^{phox}) or control isotype-matched IgG1 mab (02-6100, ThermoFisher Scientific, Illkirsh, France) for 30 min on ice. The cells were washed twice and incubated with Alexa-Fluor-488 goat-F(ab)$_2$ anti-mouse IgG1 (A11070, Invitrogen, Villebon sur Yvette, France) for 30 min on ice. After two washes as above, the cells were incubated with 2.5 µg/mL Alexa Fluor 647 rat anti-human CD294 (CRTH2, BD Biosciences, Pont de Claix, France) for 30 min on ice and washed [28]. Cell-associated fluorescence (FL1 and FL4) was measured on 100,000 events. Data were collected and analyzed with the FACS DIVA software and FlowJo software-Tree Star (BD Biosciences, Pont de Claix, France).

Western blot

Expression of NOX2, p22^{phox}, p47^{phox}, p67^{phox} and p40^{phox} in a 1% Triton X100 soluble extract prepared from human neutrophils was examined by Western blot analysis using monoclonal antibodies anti-NOX2 48 and anti-p22^{phox} 449 [42-44] polyclonal antibodies anti-p67^{phox} (C19, SC7662, Santa Cruz), anti-p47^{phox} and anti-p40^{phox} [45, 46]. Polyclonal anti-gG-HRP was used as a second antibody and the immune complexes were detected by chemiluminescence using an ECL kit Femtomax (Rockland Immunochemicals, Limerick, PA, USA). Protein concentration was determined by Pierce BCA Protein Assay^{TM} Kit (ThermoFisher, Illkirsh, France) [47].

Molecular analysis

Preparation of RNA and DNA

Total RNA was isolated from either mononuclear cells or EBV transformed B lymphocytes of both CGD patients and healthy individuals, using a modified single-step method [48]. Genomic DNA was purified with a purification kit (ref 51206 Flexigene DNA kit, Qiagen, Hilden, Germany).

Sequencing

When possible, first-strand cDNA was synthesized from total RNA by reverse transcriptase reaction according to the manufacturer's instructions (ref 11EMAMV203, MP Biomedicals Santa Ana, CA, USA). Total cDNA was immediately amplified by PCR in three overlapping PCR fragments and separated by gel electrophoresis [49]. The bands were photographed under UV (GelDoc XR+Biorad, Marnes-la-Coquette, France). All PCR products were sequenced using an ABI 3730 XL 96 capillary sequencer (Perkin Elmer, Foster City, CA, USA). More than 500 sequences of control cDNA of NOX2 were analyzed to rule out the possibility of polymorphisms. In all cases, location of mutations found in cDNA was verified in *CYBB* genomic DNA after PCR amplification of

each exon and flanking intron regions using appropriate forward and backward primers [[49]], followed by Sanger sequencing. This was done for all patients except for P1, P4a and P12. For patient P1 we used primers to amplify the promoter region of *CYBB* as previously described [28]. For patients P4a and P12 new primers were designed to amplify a partial sequence of intron 3 (I3F-GAG AGT CTG AGT CAT TGC TCA G; I3R-CTA TCC GGA AGG TGG TCA TAG) and introns 8 and 9 (I8F-GCG ACA GAG GCA TTA TTT GGT T; I9R-CCT ATG TCT TGC CAG GAC ATC) of *CYBB*, respectively. Aliquot of all PCR products in bromophenol blue solution were run together with a DNA ladder (ref R0211, ThermoFisher scientific, Illkirch, France) on 1.5% (wt/vol) agarose containing Gel Red™ nucleic acid stain (ref 41003, Biotium, Inc, Fremont, CA, USA) in parallel with a negative control (PCR products amplified without DNA) and a positive control (PCR amplification of control DNA) to analyze size and purity. In some cases, PCR products were purified from agarose gel according to manufacturer instruction (QIAquick Gel Extraction kit, ref 28704, Qiagen, Courtaboeuf, France).

Directed mutagenesis and stable transfection into X-CGDPLB-985 cells

Thr208Arg and Thr503Ile point mutations were introduced into the wild-type (WT) NOX2 cDNA in pBluescript II KS(+) vector using the QuikChange site-directed mutagenesis kit (Stratagene, San Diego, CA, USA) according to the manufacturer's instructions. The sequence of WT and the mutated NOX2 cDNA were verified by dideoxynucleotide sequencing. The WT or mutant NOX2 cDNAs were subcloned into the mammalian expression vector pEF-PGKneo and electroporated into X-CGD PLB-985 cells in which the *CYBB* gene was disrupted by gene targeting, resulting in the absence of Nox2 expression and NADPH oxidase activity, as previously described [33]. Clones expressing WT or mutated NOX2 were selected by limiting dilution in 1.5 mg/mL geneticin**.**

Results

Sum up of clinical data

X-CGD patients were diagnosed from the age of one month (P6) to 26 years (P4a), but 10 patients out of 16 were diagnosed before the age of 2. The most frequent feature was prolonged fever, skin abscesses, adenopathies and pulmonary infections (Table 1). Some patients suffered from an inflammatory syndrome in the gastrointestinal tract (P2, P3, P4a, and P8). Patients P3, P8, P9 and P16 suffered from liver abscesses. The criteria of severity were defined according to the presence of severe infections in deep organs (lung, liver, bone…) associated with sepsis, and the age of first symptoms. Tissues examination of some patients (P2, P3, and P8) showed granuloma in skin, liver or tonsils. Patients P1, P4a, P7 and P10 suffered from skin infections and gastroenteritis only without infections in deep organs. Patient P1 was diagnosed at the age of 2 when he suffered from mild infections in the skin. A splenomegaly was detected at the time of diagnosis. He is now in good health under prophylactic treatment. Patient P4a had no susceptibility to infections during childhood and adolescence. He suffered from pollen allergy and mild asthma but he received no regular medication (Table 1). At the age of 13 he had recurrent perianal abscesses and fistulas. Crohn disease was suspected. In 2012 he had mild *S. aureus* infection around his nose. He was diagnosed at 26 years of age at the time of the death of his younger brother P4b from sudden-onset *Aspergillus pneumonitis*. P4a has been symptom-free for years and he's now in good health under prophylactic treatment. Patient P7 had only superficial adenopathies and infections but was febrile

and suffered from cyanosis and hypothermia. Six patients out of 16 suffered from sepsis or prolonged fever (P2, P6, P9, P10, P12, and P15) and one had a permanent hyperthermia (P2). *S. aureus* was the most frequently encountered bacterium (P2, P4a, P7, P10 and P14), *S. marcescens* being also found two times (P2, P3). Other bacteria were detected often at the origin of infections in CGD patients, such as *S. typhimurium* and *K. pneumonia, which* were found only in patient P12, *Mycobacterium bovis* in patient P11 and *Streptococcus spp* in patients P5 and P12. Pulmonary aspergillosis was found in patients P4a and P12, and suppurative inguinal adenopathies with *C. albicans* in P12 and at *S. aureus* in P10. Regarding the oldest patients P4a, P12 and P14, two of them were diagnosed early (P12 and P14) while patient P4a was diagnosed at the age of 26. This late diagnosis correlates perfectly with the level of severity of the disease (Table 1). This will be discussed according to the CGD subtypes these patients suffer from.

With respect to the treatment of CGD patients, all had a prophylactic life-long treatment (trimethoprim/sulfamethoxazole/itraconazole). Permanent corticosteroid therapy at low-dose was given to patients P2 and P14 because of a permanent hyperthermia and inflammatory syndrome (P2), and permanent respiratory failure required permanent oxygen therapy (P14). Four patients (P5, P8 P9 and P16) had bone marrow precursor cell transplantation at the age of 16 months to four years. Three patients have complete chimerism (P5, P9 and P16). Patient P5 suffered from chronic joint GvH, P16 had an acute digestive GvH and patient P8 had persistent diarrhea six-month post-transplant. Patient P9 is currently in good health.

Phenotypic and genotypic characterization of X-CGD patients

The NADPH oxidase activity of purified neutrophils from the 16 X-CGD patients and their relatives was measured by several different methods (as described in Materials and methods) and appeared totally abolished except for patients P1 and P4a (Table 2). We underline that the NADPH oxidase activities measured by the NBT reduction test correlate perfectly with those obtained by flow cytometry with the DHR probe in all the patients' neutrophils. In addition, for the mothers (M1-2, M4, M5, M8, M10-11, and M16) the percentage of "oxidase positive" neutrophils correlates perfectly with the percentage of neutrophils presenting a normal expression of NOX2, measured by flow cytometry (Table 2, Fig. 1a). We confirm the large variation in the mothers' phenotype due to different X inactivation patterns. Only one mother was not carrier of the disease of her son (M7) (Fig. 1a) but we did not investigate the mothers of patients P13 and P14. The daughter of patient P14 was diagnosed as a carrier as well (Table 2). In some cases, the absence of NADPH oxidase activity found in patients was measured by SOD-sensitive cytochrome *c* reduction (P6, P12, and P15) or resorufin oxidation (P3, P6, P14), which measures external production of superoxide ($O_2^{\cdot-}$) or hydrogen peroxide (H_2O_2), respectively (Table 2). However, these methods are less useful to detect a carrier status of mothers because the two populations of cells (oxidase-positive and -negative populations) cannot be distinguished by these methods. We also investigated the carrier status of maternal aunts, great-aunts and grandmothers too by looking for the genetic mutation found in the index X-CGD patients (Gm2, Gam5, Am6, and Am15). None was carrier. Some sisters of X-CGD patients (S4 and S12) were carriers, whereas S8 seemed not to be carrier regarding the NADPH oxidase activity. However, S8 was not fully investigated (no genetic analysis) because she was healthy and under-age for genetic diagnosis (to sign informed consent). For B12, the brother of P12, we tested only the NADPH oxidase activity in his neutrophils for the same reason as S8. Patient P12 was classified as an $X91^{0-}$CGD patient because of the total absence of NOX2 and p22phox expression by western blotting (Fig. 1b). However normal NOX2 and $p22^{phox}$

expression was found in patient P15's neutrophils even in absence of NADPH oxidase activity (Fig. 1c). The equal expression of cytosolic factors $p40^{phox}$, $p47^{phox}$ and $p67^{phox}$ in all the samples can be considered as an internal control of protein loading. This is a typical profile of an $X91^{+}$-CGD sub-type. In addition, for patients P1 and P4a, a faint NADPH oxidase activity and a low NOX2 and $p22^{phox}$ expression were found that is typical for $X91^{-}$-CGD subtypes (Table 2). These cases will be discussed according to their specific genetic mutation.

$X91^{0}$-CGD patients

Thirteen of 16 X-linked CGD patients suffered from $X91^{0}$-CGD except patients P1, P4a ($X91^{-}$-CGD) and P15 ($X91^{+}$-CGD). Indeed, neither NADPH oxidase activity nor NOX2 and $p22^{phox}$ expression were found in the neutrophils of these 13 X^{0} CGD patients (Table 2, Fig. 1a and b, Fig. 3a, b and c). Among these 13 patients we found four missense mutations, three small deletions, two nonsense mutations, one small insertion, one large deletion, one duplication and one splice mutation. The new double missense mutation c.637 C>G (exon 6) and c.1522 C>T (exon 12) leading p.Thr208Arg and p.Thr503ILeu mutations in NOX2 respectively (patient P6), are responsible for a $X91^{0}$-CGD phenotype (Fig. 3a, b and c). This case is extremely rare in CGD [4]. Each of these last missense mutations was deleterious for the NADPH oxidase activity but not for its expression. In order to discard a possible polymorphism, we studied the functional impact of each mutation in the NOX2 knock-out PLB-985 cell line, as we previously did. Using directed mutagenesis and stable transfection in this cellular model, we found that each mutation (p.Thr208Arg and p.Thr503ILe) was deleterious for the NADPH oxidase activity (Fig. 3e), whereas only p.Thr208Arg mutation leads to the absence of NOX2 expression (Fig. 3 d). However, we can conclude that neither mutation is a polymorphism. His mother is heterozygous for each mutation. The structural impact of each mutation will be discussed in the context of a 3D dehydrogenase model of NOX2 (Fig. 2 a and b) [37].

$X91^{+}$-CGD patients

Among 681 X-linked CGD cases reported in 2010 [4] only 38 patients with 28 different mutations were identified as having an $X91^{+}$-CGD sub-type. Often, these CGD variants are due to missense mutations [19]. The phenotype of Patient P15's neutrophils fit perfectly with this type of variant (Table 2). Indeed, all the NADPH oxidase sub-units were normally expressed in P15's neutrophils (Fig. 1c), whereas the NADPH oxidase activity was totally abolished (Table 2). A point mutation in exon 10 of *CYBB* (c.1235G>A) was responsible for the change of glycine-412 to glutamic acid in NOX2 (p.Gly412Glu) (patient P15) (Fig. 2a and b). The total absence of NADPH oxidase activity correlates with the severe clinical profile found of this patient (Table 1). This mutation was reported in Roos et al., 2010b, but not fully characterized. Gly412 is in the dehydrogenase domain of NOX2 close to the NADPH binding site (Fig. 1). This will be discussed in the context of a 3D dehydrogenase model of NOX2 (Fig. 2b) [37].

$X91^{-}$-CGD patients

A faint but significant NADPH oxidase activity was detected in the neutrophils of patients P1 and P4a (Table 2). The pattern of NOX2 expression was different in both patients. In patient P1, 97% of the neutrophils exhibited no NADPH oxidase activity, whereas about 3% of cells had a normal oxidase activity related to a normal expression of NOX2 (Table 2, Fig. 4a). This small population of cells was identified as eosinophils thanks to a CD294 double staining. However, a CD294 positive and oxidase negative population of cells was also highlighted (Fig. 4a). CD294, also named CRTH2, is a seven-transmembrane G-protein-coupled receptor known as the chemoattractant receptor-homologous molecule expressed also in Th2 cells. Thus, maybe these cells were lymphocytes. The level of NOX2 expression is also in accordance with the percentage of both populations of

cells (neutrophils and eosinophils) (Fig. 4b). NOX2 expression and the cytochrome b_{558} spectrum of patient P1's cells are probably due to eosinophilic contamination of the neutrophils after Ficoll purification (Fig. 4c and d). Using the same amount of proteins for each sample (control, mother and patient P1) (20 µg) loaded on the SDS-PAGE, a faint NOX2 and $p22^{phox}$ expression in patient P1's granulocytes was seen by western blot analysis (Fig.4c). We verified that NOX2 was correctly glycosylated by performing a western blot with 200 µg of protein for patient P1 (data not shown). A novel -67delT mutation was found in the promoter region of *CYBB* (Fig. 4e). This point mutation is located in a region between the CCAAT and the TATA boxes in a consensus binding region of transcription factors (TFs) of the ets family (Elf1 and PU.1) [29, 50, 51] (Fig. 4f). Others and we previously demonstrated that mutations located in this region disturb the binding of these TFs, which are necessary to trigger NOX2 expression [25, 26, 28]. However, in eosinophils, NOX2 expression is not under the control of these TFs [52]. This explains the NOX2 expression and the NADPH oxidase activity seen in the eosinophils of patient P1 (Fig. 4a and b).

For patient P4a, we found that the whole population of neutrophils exhibited a faint NADPH oxidase activity (Fig. 5a). This result correlates with the faint formazan staining of patient P4a's neutrophils in the NBT reduction test (Fig. 5b). A low NOX2 expression was also found in patient P4a's neutrophils by flow cytometry and western blot analysis, which correlates with the level of NADPH oxidase activity found in these cells (Fig. 5c and d). In addition, a substantial $p22^{phox}$ expression was found in patient P4a's neutrophils, but in fewer amounts than in control neutrophils (Fig. 5e). His mother and his sister seemed to be carriers because they both possessed two populations of neutrophils, one oxidase-positive and an oxidase-negative population. This distribution was also seen in the NBT reduction test (Fig. 5b). However, the percentage of each population differs in the mother and the sister of patient P4a (Fig. 5a). His mother has a major population of neutrophils with a normal oxidase activity (80% of the neutrophils) and the remaining neutrophils have a slight oxidase activity as seen in her son (20% of neutrophils), even in presence of catalase. In contrast, his sister has about 50% of neutrophils with a normal oxidase activity and 50% of cells with no oxidase activity (Table 2, Fig. 5a). This distribution is confirmed by the NOX2 and $p22^{phox}$ expression profiles in their neutrophils (Fig. 5d and e). These differences are probably caused by different X inactivation patterns in both carriers.

To find the mutation in *CYBB* of patient P4a, NOX2 cDNA was amplified in 3 overlapping fragments from total mRNA by RT-PCR. Two bands were found in the first amplified fragment (β1-β2), one having a normal size (621 bp) corresponding to exon 1 to exon 6, the other having an abnormal higher size. Each band was excised, and cDNA was purified and sequenced. No mutation was found in the normal-sized band (exon 1 to exon 6). The sequence of the upper band showed an insertion of 124 bp of intron 3 as described in Table 2 and Fig. 5f. No mutations were found in the two other amplified fragments of cDNA (β3-β4 and β5-β6). We sequenced all exons of *CYBB* with intronic flanking regions after PCR amplification from the genomic DNA of patient P4a and his relatives and no mutation was found. Then intronic regions surrounding the inserted region of intron 3 was amplified and sequenced. A novel c.253-1879A>G hemizygous mutation was found that activates a splicing donor site. The inclusion of the 124-bp fragment into the mRNA unveils an active cryptic acceptor site at the start of a pseudo-exon, and this inclusion is responsible for the partial loss of the NOX2 expression (Fig. 5f). Bioinformatic analysis allows the estimation of the splice donor sequence strength. The c.253-1879A>G mutation induces increase of the splice donor strength from 6.02 to 9.14 with the MaxEntScan matrix and from 83.52 to 95.58 with the HSF matrix (http://www.umd.be/HSF/technicaltips.html). The inserted sequence in the

NOX2 cDNA creates a frameshift and introduction of a stop codon at position 85, explaining the loss of NOX2 expression (Fig. 5f). However, the neutrophils of patient P4a exhibited a low NOX2 expression related to a low NADPH oxidase activity by flow cytometry; it seems that a faint amount of normal NOX2 was expressed in his cells. The c.253-1879A>G mutation was also found in the genomic DNA of his mother and his sister in one allele, confirming their carrier status.

In conclusion, patients P1 and P4a suffer from an $X91^-$-CGD but the genetic mutation is very different for both patients, which can explain phenotypic differences in their neutrophils. According to their clinical data, both patients suffer from a mild form of CGD.

Discussion

We reported here 16 patients with X-linked CGD (X91-CGD, OMIM #306400) presenting mutations in the *CYBB* gene. Most of the patients were from France except patients P4a, P11 and P13 who came from Finland, Lithuania and Croatia respectively. Most of the patients suffered from an $X91^0$-CGD, except patient P15 who had an $X91^+$-CGD and patients P1 and P4a who exhibited an $X91^-$-CGD. This classification is based on the level of NOX2 expression as previously demonstrated. All types of mutations were found leading to $X91^0$-CGD type and 6 out of 13 were new and spread over the whole coding region. Two out of these 6 new $X91^0$-CGD mutations were a point mutation in intron 6 (patient P7) and a large deletion (intron 9/exon 9) (patient P12) leading to the deletion of exons 5/6 and exon 9, respectively. Regarding their clinical signs, the $X91^0$-CGD cases were as far the most severe forms probably because of the absence of NOX2 expression and NADPH oxidase activity. The severity of the impact of missense mutations on the NADPH oxidase expression and activity can be highlighted regarding their effect on the structure of the enzyme. Indeed we analyzed an extremely rare case of $X91^0$-CGD due to a double missense mutation (p.Thr208Arg and p.Thr503ILeu). To our knowledge it is the first listed case of a double missense mutation causing a $X91^0$-CGD. We previously published a unique case of a similar double missense mutation p.His303Asn/Pro304Arg leading to an $X91^+$-CGD sub-type ([53, 54]). Each missense mutation was deleterious for the NADPH oxidase activity but not for its expression ruling out the possibility of a polymorphism. However, polymorphisms are rare in *CYBB* [4]. In the present case, and regarding their respective position in the NOX2 model, each mutation acts through different mechanisms. Thr208 is located in the transmembrane segment V just upstream of His209, which is one of the proximal heme ligands (Fig. 2a). Thus, the mutation in the transmembrane domain of this Thr208 to an Arginine, cumulating higher steric properties and a positive charge, may be deleterious to the structure of the transmembrane domain and at least locally may impair proper orientation of His209. This may lead in cascade to the absence of proximal heme and thus the impossibility to mature the final protein explaining a $X91^0$ phenotype for this modeled single mutant. Regarding Thr503ILe, the second cumulative missense mutation in this patient, its modelling in PLB985 leads to a normal expression but the loss of activity and thus a $X91^+$ phenotype. This Thr503 is located in a hot spot for $X91^+$-CGD mutations in the NIS (NOX Insertion sequence), which is a sequence specific of NOX dehydrogenase domains but absent in other structurally related dehydrogenase domain (e.g. ferredoxin $NADP^+$ reductase) (Fig. 2b). Previous mutations reported in the NIS have been shown to impair assembly with cytosolic factor and/or activation or the initial electrons transfer from NADPH to FAD [33-35]. Regarding to its location, the Thr503ILe mutation is likely to induce similar defect to those already studied and characterized in this NIS. [37]. Among missense mutations in *CYBB* (Fig. 1a), the p.Val327Asp mutation leading to a $X91^0$-CGD in NOX2 was new. This Val residue is located in the FAD binding subdomain of the NOX2 dehydrogenase domain (Fig.

2b) and is at the center of a hydrophobic cluster within the domain. Introducing an aspartic acid in that position (Fig. 2b) is expected to disorganize the structure of the domain. This is fully compatible with the $X91^0$ phenotype within patient P10. Similar analysis can be drawn for the Trp516Arg mutant, where the Trp516 side chain is at the center of a hydrophobic cluster within the NADPH binding subdomain (Fig. 2b). Its replacement by an Arg residue do not allow the correct folding.

Replacement of Gly412 by a glutamic acid lead to a rare $X91^+$ phenotype. At this position in the structure a glycine residue is strictly conserved, as well in the neighboring loops containing G408 and G538 (Fig. 2b). Addition of a Glu in this position may distort the proper packing of the Rossman fold and thus an efficient NADPH binding site. In addition, a Glu in this position adds a negative charge in the heart of the NADPH binding site which is already a strongly negatively charged coenzyme. These various elements explain a defective recognition of NADPH in such Gly412Glu mutant [37]. However, the clinical feature of this $X91^+$-CGD was as severe as $X91^0$-CGD cases because of the total absence of NADPH oxidase activity in phagocytes. The clinical severity of $X91^-$-CGD is variable and depends on the localization of the mutations in *CYBB* related to the level of NADPH oxidase activity found in patients' phagocytes [19, 22, 24]. This $X91^-$-CGD variant is often due to missense mutations, small deletions or insertions in the encoding region of NOX2 (52 cases of $X91^-$-CGD listed in [4] leading to a decrease of its expression in phagocytes, the NADPH oxidase activity being slightly or totally abolished. We previously demonstrated that there are two categories of $X91^-$-CGD mutations, one in which the NADPH oxidase activity is proportional to the NOX2 expression level and another one showing an absence of NOX activity associated with variable levels of NOX2 expression, the last one being associated with more severe clinical cases [22]. This work also permitted to point out potential binding regions of NOX2 with $p22^{phox}$, essential for normal synthesis of cytochrome b_{558}. In this work, the impact of the point mutation in intron 3 of *CYBB* on NOX2 expression and NADPH oxidase activity in phagocytes of patient P4a, was quite unusual. Indeed, a unique population of neutrophils was found by flow cytometry characterized by a faint NOX2 expression associated with a low NADPH oxidase activity, suggesting that normal mRNA was present in phagocytes. Indeed, even if mutated mRNA can be removed by Nonsense-Mediated mRNA Decay, the normal splice manages to remain in the patient P4a's neutrophils. In addition, $p22^{phox}$ expression was faintly impacted by this mutation. Thus, the clinical form of this $X91^-$-CGD case was mild. The faint but substantial NADPH oxidase activity found in the neutrophils' population of patient P4a could partially protect him against infections. However, we must also underline that patient P4a had a younger brother P4b who died at 24 years of age of sudden onset *Aspergillus* pneumonitis. CGD was suspected post mortem for patient P4b and no biological investigation was done for him. Patient P4a was diagnosed after his brother´s death. He is in good health and he is now a father for two children. Patient P1 suffered from a mild clinical form as it was the case for the other patients with this type of mutation [25, 26, 28]. Only five different mutations in the *CYBB* promoter leading to $X91^-$-CGD were documented in the literature [for review see [23]. Location of these mutations is situated in a region between the CCAAT and the TATA boxes in a consensus-binding region of transcription factors of the ets family (Elf1 and PU.1) that regulate NOX2 expression in neutrophils and monocytes [29, 50, 51]. However, NOX2 expression is regulated differently in eosinophils [52] explaining that patient P1 can partially be protected again infections because of the normal NADPH oxidase activity in his eosinophils.

In conclusion, in addition to rapid and efficient diagnosis provided by the new generation of high-throughput sequencing, certain rare monogenic disease like CGD requires complete functional and molecular

investigation to better understand the impact of each genetic mutation on the enzyme expression and activity related to the clinical severity of the disease. This refined characterization helps to understand the molecular mechanisms of the disease and to some extent may assist in the care and follow-up of these patients. In addition, thanks to the 3D model of the dehydrogenase domain of NOX2 and the functional study of single mutation in the NOX2 knock-out PLB-985 cell line, the analysis of the impact of certain CGD missense mutations on NOX2 activity and synthesis, permits to improve our knowledge of the functioning of this enzyme.

Acknowledgements

M. M., S. B., B. V. and J. B. performed the functional and molecular analysis; N. R-B., J. R. and J. F. performed the DNA sequencing, V. B., G. C., C. D., F. F., V. G., M. R., J-P. B., C. B-B, E. J., L. E., C. J., S. D. H., M H-C., M. H., G. M., Y. B., D. P., J. K., R. T., and L. K., did the clinical diagnosis and collected the clinical data; D. M. collected some functional data; F. F. contributed to the analysis of data, drew Fig 1(b) and revised the article; M. J. S. carried out the conception and the design of the study, the acquisition, the analysis and the interpretation of data and the drafting of the article.

I would like to pay tribute to Cécile Martel who was largely involved in the diagnosis of CGD patients for more than thirty years and who passed away in 2016. A warm thank to Prof Dirk Roos, The Netherland, for his careful rereading, corrections and judicious advices.

MJS is grateful for supports from the University Grenoble Alpes (UGA) (AGIR program 2014); the Faculty of Medicine Grenoble, Interreg France-Suisse [Programme de Cooperation Territoriale Européenne, Fond Européen de Développement Regional (FEDER), 2017–2019]. This work was also supported by the Delegation for Clinical Research and Innovations, University Hospital Grenoble Alpes (CHUGA) (DRCI, Rementips project 2014).

Conflict of interest

On behalf of all authors, the corresponding author states that there is no conflict of interest.

References

1. Mahlaoui N, Picard C, Bach P, Costes L, Courteille V, Ranohavimparany A, *et al.* Genetic diagnosis of primary immunodeficiencies: A survey of the French national registry. *J Allergy Clin Immunol* 2019,**143**:1646-1649 e1610.
2. Roos D. Chronic granulomatous disease. *Br Med Bull* 2016,**118**:50-63.
3. Roos D, Kuhns DB, Maddalena A, Bustamante J, Kannengiesser C, de Boer M, *et al.* Hematologically important mutations: The autosomal recessive forms of chronic granulomatous disease (second update). *Blood Cells Mol Dis* 2010.
4. Roos D, Kuhns DB, Maddalena A, Roesler J, Lopez JA, Ariga T, *et al.* Hematologically important mutations: X-linked chronic granulomatous disease (third update). *Blood Cells Mol Dis* 2010.
5. van de Geer A, Nieto-Patlan A, Kuhns DB, Tool AT, Arias AA, Bouaziz M, *et al.* Inherited p40phox deficiency differs from classic chronic granulomatous disease. *J Clin Invest* 2018,**128**:3957-3975.
6. Yu L, DeLeo FR, Biberstine-Kinkade KJ, Renee J, Nauseef WM, Dinauer MC. Biosynthesis of flavocytochrome b558 . gp91(phox) is synthesized as a 65-kDa precursor (p65) in the endoplasmic reticulum. *J Biol Chem* 1999,**274**:4364-4369.
7. Nauseef WM, Clark RA. Intersecting Stories of the Phagocyte NADPH Oxidase and Chronic Granulomatous Disease. *Methods Mol Biol* 2019,**1982**:3-16.
8. Thomas DC, Charbonnier LM, Schejtman A, Aldhekri H, Coomber EL, Dufficy ER, *et al.* EROS/CYBC1 mutations: Decreased NADPH oxidase function and chronic granulomatous disease. *J Allergy Clin Immunol* 2019,**143**:782-785 e781.
9. Gu Y, Williams DA. RAC2 GTPase deficiency and myeloid cell dysfunction in human and mouse. *J Pediatr Hematol Oncol* 2002,**24**:791-794.

10. Yu H, Leitenberg D, Li B, Flavell RA. Deficiency of small GTPase Rac2 affects T cell activation. *J Exp Med* 2001,**194**:915-926.
11. Roberts AW, Kim C, Zhen L, Lowe JB, Kapur R, Petryniak B, *et al.* Deficiency of the hematopoietic cell-specific Rho family GTPase Rac2 is characterized by abnormalities in neutrophil function and host defense. *Immunity* 1999,**10**:183-196.
12. Sharapova SO, Haapaniemi E, Sakovich IS, Kostyuchenko LV, Donko A, Dulau-Florea A, *et al.* Heterozygous activating mutation in RAC2 causes infantile-onset combined immunodeficiency with susceptibility to viral infections. *Clin Immunol* 2019,**205**:1-5.
13. Hsu AP, Donko A, Arrington ME, Swamydas M, Fink D, Das A, *et al.* Dominant activating RAC2 mutation with lymphopenia, immunodeficiency, and cytoskeletal defects. *Blood* 2019,**133**:1977-1988.
14. Williams DA, Tao W, Yang F, Kim C, Gu Y, Mansfield P, *et al.* Dominant negative mutation of the hematopoietic-specific Rho GTPase, Rac2, is associated with a human phagocyte immunodeficiency. *Blood* 2000,**96**:1646-1654.
15. Ambruso DR, Knall C, Abell AN, Panepinto J, Kurkchubasche A, Thurman G, *et al.* Human neutrophil immunodeficiency syndrome is associated with an inhibitory Rac2 mutation. *Proc Natl Acad Sci U S A* 2000,**97**:4654-4659.
16. Sumimoto H. Structure, regulation and evolution of Nox-family NADPH oxidases that produce reactive oxygen species. *Febs J* 2008,**275**:3249-3277.
17. van den Berg JM, van Koppen E, Ahlin A, Belohradsky BH, Bernatowska E, Corbeel L, *et al.* Chronic granulomatous disease: the European experience. *PLoS One* 2009,**4**:e5234.
18. Winkelstein JA, Marino MC, Johnston RB, Jr., Boyle J, Curnutte J, Gallin JI, *et al.* Chronic granulomatous disease. Report on a national registry of 368 patients. *Medicine (Baltimore)* 2000,**79**:155-169.
19. O'Neill S, Brault J, Stasia MJ, Knaus UG. Genetic disorders coupled to ROS deficiency. *Redox Biol* 2015,**6**:135-156.
20. Royer-Pokora B, Kunkel LM, Monaco AP, Goff SC, Newburger PE, Baehner RL, *et al.* Cloning the gene for the inherited disorder chronic granulomatous disease on the basis of its chromosomal location. *Cold Spring Harb Symp Quant Biol* 1986,**51 Pt 1**:177-183.
21. Teahan C, Rowe P, Parker P, Totty N, Segal AW. The X-linked chronic granulomatous disease gene codes for the beta-chain of cytochrome b-245. *Nature* 1987,**327**:720-721.
22. Beaumel S, Grunwald D, Fieschi F, Stasia MJ. Identification of NOX2 regions for normal biosynthesis of cytochrome b558 in phagocytes highlighting essential residues for p22phox binding. *Biochem J* 2014,**464**:425-437.
23. Stasia MJ, Li XJ. Genetics and immunopathology of chronic granulomatous disease. *Semin Immunopathol* 2008,**30**:209-235.
24. Kuhns DB, Alvord WG, Heller T, Feld JJ, Pike KM, Marciano BE, *et al.* Residual NADPH oxidase and survival in chronic granulomatous disease. *N Engl J Med* 2010,**363**:2600-2610.
25. Newburger PE, Skalnik DG, Hopkins PJ, Eklund EA, Curnutte JT. Mutations in the promoter region of the gene for gp91-phox in X-linked chronic granulomatous disease with decreased expression of cytochrome b558. *J Clin Invest* 1994,**94**:1205-1211.
26. Weening RS, De Boer M, Kuijpers TW, Neefjes VM, Hack WW, Roos D. Point mutations in the promoter region of the CYBB gene leading to mild chronic granulomatous disease. *Clin Exp Immunol* 2000,**122**:410-417.
27. Stasia MJ, Brion JP, Boutonnat J, Morel F. Severe clinical forms of cytochrome b-negative chronic granulomatous disease (X91-) in 3 brothers with a point mutation in the promoter region of CYBB. *J Infect Dis* 2003,**188**:1593-1604.
28. Defendi F, Decleva E, Martel C, Dri P, Stasia MJ. A novel point mutation in the CYBB gene promoter leading to a rare X minus chronic granulomatous disease variant -- Impact on the microbicidal activity of neutrophils. *Biochim Biophys Acta* 2009.
29. Voo KS, Skalnik DG. Elf-1 and PU.1 induce expression of gp91(phox) via a promoter element mutated in a subset of chronic granulomatous disease patients. *Blood* 1999,**93**:3512-3520.
30. Zhen L, King AA, Xiao Y, Chanock SJ, Orkin SH, Dinauer MC. Gene targeting of X chromosome-linked chronic granulomatous disease locus in a human myeloid leukemia cell line and rescue by expression of recombinant gp91phox. *Proc Natl Acad Sci U S A* 1993,**90**:9832-9836.
31. Yu L, Cross AR, Zhen L, Dinauer MC. Functional analysis of NADPH oxidase in granulocytic cells expressing a delta488-497 gp91(phox) deletion mutant. *Blood* 1999,**94**:2497-2504.
32. Zhen L, Yu L, Dinauer MC. Probing the role of the carboxyl terminus of the gp91phox subunit of neutrophil flavocytochrome b558 using site-directed mutagenesis. *J Biol Chem* 1998,**273**:6575-6581.

33. Li XJ, Grunwald D, Mathieu J, Morel F, Stasia MJ. Crucial role of two potential cytosolic regions of Nox2, 191TSSTKTIRRS200 and 484DESQANHFAVHHDEEKD500, on NADPH oxidase activation. *J Biol Chem* 2005,**280**:14962-14973.
34. Li XJ, Fieschi F, Paclet MH, Grunwald D, Campion Y, Gaudin P, *et al.* Leu505 of Nox2 is crucial for optimal p67phox-dependent activation of the flavocytochrome b558 during phagocytic NADPH oxidase assembly. *J Leukoc Biol* 2007,**81**:238-249.
35. Debeurme F, Picciocchi A, Dagher MC, Grunwald D, Beaumel S, Fieschi F, *et al.* Regulation of NADPH oxidase activity in phagocytes: relationship between FAD/NADPH binding and oxidase complex assembly. *J Biol Chem* 2010,**285**:33197-33208.
36. Picciocchi A, Debeurme F, Beaumel S, Dagher MC, Grunwald D, Jesaitis AJ, *et al.* Role of putative second transmembrane region of Nox2 protein in the structural stability and electron transfer of the phagocytic NADPH oxidase. *J Biol Chem* 2011,**286**:28357-28369.
37. Beaumel S, Picciocchi A, Debeurme F, Vives C, Hesse AM, Ferro M, *et al.* Down-regulation of NOX2 activity in phagocytes mediated by ATM-kinase dependent phosphorylation. *Free Radic Biol Med* 2017,**113**:1-15.
38. Boyum A. A one-stage procedure for isolation of granulocytes and lymphocytes from human blood. General sedimentation properties of white blood cells in a 1g gravity field. *Scand J Clin Lab Invest Suppl* 1968,**97**:51-76.
39. Batot G, Paclet MH, Doussiere J, Vergnaud S, Martel C, Vignais PV, *et al.* Biochemical and immunochemical properties of B lymphocyte cytochrome b558. *Biochim Biophys Acta* 1998,**1406**:188-202.
40. Tucker KA, Lilly MB, Heck L, Jr., Rado TA. Characterization of a new human diploid myeloid leukemia cell line (PLB-985) with granulocytic and monocytic differentiating capacity. *Blood* 1987,**70**:372-378.
41. Martel C, Mollin M, Beaumel S, Brion JP, Coutton C, Satre V, *et al.* Clinical, functional and genetic analysis of twenty-four patients with chronic granulomatous disease - identification of eight novel mutations in CYBB and NCF2 genes. *J Clin Immunol* 2012,**32**:942-958.
42. Verhoeven AJ, Bolscher BG, Meerhof LJ, van Zwieten R, Keijer J, Weening RS, *et al.* Characterization of two monoclonal antibodies against cytochrome b558 of human neutrophils. *Blood* 1989,**73**:1686-1694.
43. Laemmli UK. Cleavage of structural proteins during the assembly of the head of bacteriophage T4. *Nature* 1970,**227**:680-685.
44. Towbin H, Staehelin T, Gordon J. Electrophoretic transfer of proteins from polyacrylamide gels to nitrocellulose sheets: procedure and some applications. *Proc Natl Acad Sci U S A* 1979,**76**:4350-4354.
45. Vergnaud S, Paclet MH, El Benna J, Pocidalo MA, Morel F. Complementation of NADPH oxidase in p67-phox-deficient CGD patients p67-phox/p40-phox interaction. *Eur J Biochem* 2000,**267**:1059-1067.
46. Stasia MJ, Mollin M, Martel C, Satre V, Coutton C, Amblard F, *et al.* Functional and genetic characterization of two extremely rare cases of Williams-Beuren syndrome associated with chronic granulomatous disease. *Eur J Hum Genet* 2013,**21**:1079-1084.
47. Smith PK, Krohn RI, Hermanson GT, Mallia AK, Gartner FH, Provenzano MD, *et al.* Measurement of protein using bicinchoninic acid. *Anal Biochem* 1985,**150**:76-85.
48. Chomczynski P, Sacchi N. Single-step method of RNA isolation by acid guanidinium thiocyanate-phenol-chloroform extraction. *Anal Biochem* 1987,**162**:156-159.
49. Bakri FG, Martel C, Khuri-Bulos N, Mahafzah A, El-Khateeb MS, Al-Wahadneh AM, *et al.* First report of clinical, functional, and molecular investigation of chronic granulomatous disease in nine Jordanian families. *J Clin Immunol* 2009,**29**:215-230.
50. Eklund EA, Luo W, Skalnik DG. Characterization of three promoter elements and cognate DNA binding protein(s) necessary for IFN-gamma induction of gp91-phox transcription. *J Immunol* 1996,**157**:2418-2429.
51. Suzuki S, Kumatori A, Haagen IA, Fujii Y, Sadat MA, Jun HL, *et al.* PU.1 as an essential activator for the expression of gp91(phox) gene in human peripheral neutrophils, monocytes, and B lymphocytes. *Proc Natl Acad Sci U S A* 1998,**95**:6085-6090.
52. Yang D, Suzuki S, Hao LJ, Fujii Y, Yamauchi A, Yamamoto M, *et al.* Eosinophil-specific regulation of gp91(phox) gene expression by transcription factors GATA-1 and GATA-2. *J Biol Chem* 2000,**275**:9425-9432.
53. Stasia MJ, Lardy B, Maturana A, Rousseau P, Martel C, Bordigoni P, *et al.* Molecular and functional characterization of a new X-linked chronic granulomatous disease variant (X91+) case with a double missense mutation in the cytosolic gp91phox C-terminal tail. *Biochim Biophys Acta* 2002,**1586**:316-330.

54. Bionda C, Li XJ, van Bruggen R, Eppink M, Roos D, Morel F, *et al.* Functional analysis of two-amino acid substitutions in gp91 phox in a patient with X-linked flavocytochrome b558-positive chronic granulomatous disease by means of transgenic PLB-985 cells. *Hum Genet* 2004,**115**:418-427.

Table 1. Clinical data of the 16 X-CGD patients

Patients	X-CGDvariants	Date of birth	Date of diagnosis	Severe clinical signs	Minor clinical signs	Actual treatments
P1	$X91^{-}$	12/22/13	01/20/15	/	Multiple abscessed skin lesions, Splenomegaly	Prophylactic[a]
P2	$X91^{0}$	11/18/12	09/24/14	Prolonged fever	Inflammatory syndrome, xanthogranuloma (*S. marcescens*), tonsil adenophlegmon (*S. aureus*), microcytic anemia due to martial deficiency, diarrhea, vomiting, rotavirus gastroenteritis	Prophylactic[a]
P3	$X91^{0}$	03/10/09	02/01/2012	Sepsis, hepato-splenomegaly hepatic granuloma	Pallor, pustulosis, inflammatory syndrome, bloody diarrhea (*Enterococcus faecium*), multiple necrotic adenopathies (*S. marcescens*), hepatic cytolysis and cholestasis, failure to thrive	Prophylactic[a]
P4a[b]	$X91^{-}$	02/04/86	10/18/2012	/	Mild childhood asthma, at teen-age recurrent perianal abscesses, treated for Crohn disease, nose infection (*S. aureus*)	Prophylactic[a]
P4b[b†]		1988	2012 post mortem	*Aspergillus* pneumonitis	/	/
P5	$X91^{0}$	07/29/12	04/01/14	Pulmonary abscesses (*St.constellatus*)	Neonatal pustular melanosis, eosinophilic pancolitis, maculo-papular skin rash	Engraftment at 3 years of age. Joint chronic graft versus host disease. Complete chimerism
P6	$X91^{0}$	03/13/09	04/28/09	Severe sepsis, three outbreaks of pneumonia	/	Prophylactic[a]
P7	$X91^{0}$	06/20/16	06/22/17	/	Cervical adenitis, febrile (*S. aureus*), papular lesions, fungal infections in the penis, hypothermia, cyanosis	Prophylactic[a]
P8	$X91^{0}$	12/08/15	05/19/16	Hepatic abcesses	Fever, inflammatory syndrome, rotavirus gastroenteritis, cervical adenopathies, granuloma of the tonsil, perforated acute otitis, Ileitis	Recent engraftment (HLA id.) with infectious complications and viral reactivation, persistent diarrhea six months post-transplant

P9	X91^{0}	10/28/12	06/02/14	Prolonged fever, liver abscesses	/	Engraftment at 3 years of age, complete chimerism. In good health
P10	X91^{0}	09/02/18	12/18/18	Bacteriemia (*St. Aureus*)	Reccurent suppurative inguinal (*St. Aureus*)	Prophylactic[a]
P11	X91^{0}	10/14/14	03/15/17	*Mycobacterium bovis* infection	Recurrent suppurative lymphadenitis, pneumonia, other pulmonary bacterial infections/	Prophylactic[a]
P12	X91^{0}	01/30/86	06/24/87	Sepsis (*S. typhimurium*), pulmonary aspergillosis	Suppurative inguinal adenopathies (*C. albicans*), furonculosis (*K. pneumoniae*), cervical adenopathy (S*treptoccocus*), balano-prepucial fistula, recurrent cold sores	Prophylactic[a]
P13	X91^{0}	09/07/13	07/20/16	Abscess of the mediastinum, bacteremia, bacterial pneumonia, suspected Noonan syndrome	Cervical lymphadenitis, BCGitis	Prophylactic[a]
P14	X91^{0}	02/16/83	12/02/10	Bone infection (*Aspergillus sp*) treated by laminectomy, permanent respiratory failure (restrictive and obstructive)	Peritonsillar abcess	Prophylactic[a] corticotherapy, hydroxychloroquine, amethopterine, permanent oxygenotherapy
P15	X91^{+}	12/19/03	09/20/09	Prolonged fever, pulmonary abcess	Cervical adenopathy, BCGititis, abscess of the anal margin, acute appendicitis, diarrhea chronic inflammation syndrome	Prophylactic[a]
P16	X91^{0}	01/21/13	06/30/16	Liver abcesses	Cervical adenitis	Engraftment at 16 months years of age, acute intestinal graft versus host disease. Bronchiolitis Obliterans Syndrome, complete chimerism

[a]Trimethoprim-sulfamethoxazole and itraconazole
[b]P4a and P4b are brothers. P4b died at 24 years old. At that time CGD diagnosis was done for him and his brother P4a.
[†]Dead patient

Table 2. Phenotypic and genotypic profiles of the 16 X-CGD patients

Patients	NBT test % of positive cells	Cyt *c* Red O_2^- nmol/min /10^6cells[a]	Resorufin H_2O_2 nmol/min/10^6cells[b]	DHR, Index (% of cells)[c]	Protein expression flow cytometry Index (% of cells) or WB	Cytb_{558} picolmol/mg proteins	cDNA nucleotide change	Gene location	Amino-acid change	CGD-type
P1	/	/	/	2.3 (98)-277 (2)	1.0 (98)-25,1 (2)	/	-67 delT	Promoter	No	X^-
M1	/	/	/	4.3 (36)-22.3 (63)	1.0 (33)-17,1 (67)	/				Carrier
P2	/	/	/	1.1 (100)	1.1 (100)	/	c.39delT	Exon 1	p.Phe13LeufsX21	X^0
M2	/	/	/	2.6 (47)-47.0 (53)	1.0 (46)-18.9 (54)	/				Carrier
Gm2	/	/	/	/	/	/				Not carrier
P3	1.0	/	0	1.0 (100)	Abs NOX2	/	c.201dupT	Exon 3	p.Leu68SerfsX34	X^0
P4a	21.0	/	/	10.4 (100)	2.3 (100)	36	c.253-1879A>G	Intron 3	Skip exon 3, p.Cys85LeufsX32	X^-
M4	80	/	/	3.4 (16)-13.4 (84)	2.8 (10)-30.0 (90)	342				Carrier
S4	58	/	/	1.2 (47)-12.4 (53)	2.2 (37)-30.0 (63)	315				Carrier
P5	0	/	/	1.0 (100)	1.0 (100)	/	c.600_603dupTTAC	Exon 6	p.Phe202LeufsX2	X^0
M5	30	/	/	8.4 (78)-49.8 (22)	1.0 (65)-55.0 (35)	/				Carrier
Am5	72	/	/	2.1 (24)-6.9 (76)	1.0 (17)-9.3 (83)	/				Carrier
Gam5	/	/	/	/	/	/				Not carrier
P6	0	0	0	/	/	0	c.623 C>G and c.1508 C>T	Exon 6 and Exon 12	p.Thr208Arg and Thr503ILe	X^0
M6	39	5.5	10.4	/	/	76				Carrier
Am6	/	/	/	/	/	/				Not Carrier
P7	0			1.3 (100)	1.3 (100)		c.674+3G>T	Intron 6	Deletion of exon 6 or exon 5 and 6, p.Asp162ThrfsX15	X^0
M7	94	/	/	57.8 (100)	44.7 (100)	/				Not carrier
P8	0	/	/	1.0 (100)	1.2 (100)	/	c.676C>T	Exon 7	p.Arg226X	X^0
M8	49	/	/	39.0 (48)-154 (52)	1.2 (49)-19.0 (51)	/				Carrier
S8[d]	94	/	/	15.5 (100)	8.3 (100)	/	/			ND[d]
P9	0	/	/	1.0 (100)	1.0 (100)	/	c.816G>A	Exon 8	p.Trp272X	X^0
M9	36	/	/	2.8 (78)-25.0 (22)	1.0 (60)-23.0 (40)	/				Carrier
Am9	90	/	/	158 (100)	12 (100)	/				Not carrier
Am9'	96	/	/	97 (100)	20 (100)	/				Not carrier
Gam9	/	/	/	63 (100)	10 (100)	/				Not carrier
P10	/	/	/	1.0 (100)	1.0 (100)	/	c.980T>A	Exon 9	Val327Asp	X^0
M10	/	/	/	46.0 (58)-244 (42)	1.0 (64)-23.0 (46)	/				Carrier
P11	0	/	/	1.0 (100)	1.0 (100)	/	c.1061_1065delATATC	Exon 9	p.His354ProfsX16	X^0
M11	12	/	/	3.5 (93)-217 (7)	1.3 (90)-44.7 (10)	/				Carrier

P12	0	0	/	/	Abs NOX2	0	c.897+1258_1151 +129del (del of 1657bp)	Intron9/Exon 9	Skip exon 9, p.Val300AspfsX4	X^0
M12	57	1.9	/	/	NOX2 diminished	39				Carrier
S12	73	5.0	/	/	NOX2 diminished	55				Carrier
B12[d]	80	10.0	/	/		103				ND[d]
P13	2	/	/	/	Abs NOX2	/	c. 1166G>A	Exon 10	p.Gly389Glu	X^0
P14	4	/	0	/	Abs NOX2 *?*	/	c.1167_1179delG CCCTTTGGCAC T	Exon 10	p.Phe391ValfsX9	X^0
D14	48	/	/	/		/				Carrier
P15	0	0	/	/	Pres NOX2	/	c.1235G>A	Exon 10	p.Gly412Glu	X^+
M15	88	14.6	/	/	/	/				Carrier
Am15	/	/	/	/	/	/				Not carrier
P16	4	/	/	1.1 (100)	1.2 (100)	/	c.1546T>C	Exon 12	p.Trp516Arg	X^0
M16	36	/	/	42 (68)-189 (32)	2.0 (69)-35.9 (31)	/				Carrier
Standard values (n=100)	90 ± 6	11.3 ± 3.3	25.7 ± 10.3	>5	40 ± 13	166 ± 30	/	/	/	/

P, patient; M, mother; Gm, grand-mother; S, sister; B, brother; D, daugther; Am, maternal aunt; Gam, maternal grand-aunt.

[a]Activation with PMA

[b]Activation with PMA

[c]MFI of activated cells/MFI resting cells (% of cells having index) or western blot 's results; Abs = Absence, Pres = Presence, Decr = Decrease

[d]Genetic analysis not done because they were safe and not of age.

In bold are new mutations in *CYBB*.

Figure Legends

Fig. 1. Phenotypic analysis of the neutrophils from X-linked CGD patients having new *CYBB* mutations. NOX2 expression of patients and their mothers' neutrophils was measured by flow cytometry as described in Materials and methods. Solid grey curve correspond to DHR loaded resting neutrophils, empty black curve correspond to DHR loaded neutrophils after PMA stimulation (**a**). For patient P12, the absence of gp91^{phox} (or NOX2) and p22^{phox} expression was shown by western blotting using the primary specific antibodie 48, 449 respectively (**b**). Note that all the sub-units of the NADPH oxidase complex are expressed in patient P15's neutrophils (X91^{+}CGD) by western blotting using specific antibodies as described in Material and methods (**c**).

Fig. 2. (**a**) Schematic representation of X-linked CGD point mutations within the NOX2 protein – New mutations are in red and known mutations are in blue. New mutations in the promoter (Patient P1) or in intron sequences (Patients P4a and P12) of *CYBB* are not represented. (**b**) NOX2 dehydrogenase model and modelisation of CGD mutations. The DH model is represented as ribbons, dark green for the NADPH binding domain -corresponding to the 3A1F pdb structure- and purple blue for the modelled FAD binding domain ([37]). NOX2 NIS, in light green, is an approximate structural model but is partly disordered, flexible as suggested by the absence of density in the 3A1F structure for this sequence. Some of the residues corresponding to X91^{0} and X91^{+} mutations are highlighted as shown in stick (V327, G412, W516, and T503). Three zooms highlight the V327, G412 and W516 residues with emphasis on the neighboring residues around the considered mutations. In each case, the mutated position is presented with both the wild type side chain and the corresponding mutation, in orange, superimposed. Molecular graphic images were produced using PyMOL software

Fig. 3 Functional analysis of patient P6's T208R and T503I substitutions in NOX2 by means of transgenic PLB-985 cells. Measurement of the NADPH oxidase activity of neutrophils of patient P6 and of his mother by resorufine oxidation (Amplex Red^{R}) after opsonized zymosan, PMA and PAF/fMLF activation as described in Materials and methods (**a**). Expression of NADPH oxidase sub-units NOX2, p67^{phox} and p47^{phox} p40^{phox} and p22^{phox} in patient P6 and his mother's neutrophils by western blot analysis (**b**). Cytochrome b_{558} differential spectra of 1% Triton X100 soluble extract from patient P6 and his mother's neutrophils (**c**). NOX2 expression in differentiated T208R-NOX2 and T503I-NOX2 transgenic PLB-985 cells by flow cytometry using the 7D5 monoclonal antibody against NOX2 and PE coupled polyclonal antibody anti IgG1 (empty black curve). Solid grey curve correspond to resting neutrophils labelled with monoclonal Mouse IgG1 isotype as an irrelevant antibody (**d**). NADPH oxidase activity of differentiated T208R-NOX2 and T503I-NOX2 transgenic PLB-985 cells measured by chemiluminescence in presence of luminol, HRPO after 80 ng/mL PMA stimulation (**e**).

Fig. 4 Phenotypic and genotypic characterisation of the X91^{-}-CGD of patient P1 due to a new point mutation in the *CYBB* promoter. Flow cytometry dot plots of NADPH oxidase activity (DHR) and CD294 expression (eosinophil marker) in neutrophils and eosinophils of granulocyte preparations from a healthy subject (bottom panels) and patient P1 (top panels) at rest (left panels) or after stimulation with PMA (right panels). Left panels correspond to dot plots of cells labelled with isotype control antibodies and loaded with DHR. (**a**). Flow cytometry dot plots of NOX2 and CD294 expression (eosinophil marker) in neutrophils and eosinophils of granulocyte preparations from a healthy subject (bottom panels) and patient P1 (top panels) using 7D5 monoclonal antibody and anti-CD294 antibody (right panels) compared to dot plots of isotype controls (left panels) (**b**). NOX2 and p22^{phox} expression in patient P1 and his mother's granulocytes by western blot analysis. A faint NOX2 and p22^{phox} expression are visible probably due to the presence of eosinophils in the granulocyte preparation (**c**). Cytochrome b_{558} differential spectra of 1% Triton X100 soluble extract from patient P1 and his mother's neutrophils (**d**). Thymidine deletion at position -67 detected in the *CYBB* promoter region of patient P1 and his mother as a carrier, compared to a healthy donor sequence (**e**). Schematic representation of part of the *CYBB* promoter region, with localization of the "CCAAT" and "TATA" boxes, the ATG starting codon and the point mutation described in panel e (**f**).

Fig. 5 Phenotypic analysis of the neutrophils of patient P4a suffering from an X91^{-}-CGD and having a new *CYBB* mutation. NADPH oxidase activity of patient P4a his sister and his mother s'neutrophils was measured by flow cytometry after stimulation during 15 min with 200 ng/mL PMA in presence of dihydrorodamine (DHR) probe as described in Materials and methods. Solid grey curve correspond to DHR loaded resting neutrophils, empty black curve correspond to DHR loaded neutrophils after PMA stimulation (**a**). The NADPH oxidase activity of patient P4a his sister and and his mother s' neutrophils was also measured using the NBT reduction test (**b**). NOX2 and p22^{phox} expression was shown by western blot using the primary specific antibodies 48 and 449 respectively (**c**). Nox2 (**d**) and p22^{phox} expression (**e**) was shown by flow cytometry using the primary specific antibodies 7D5 and 449 respectively. Solid grey curve correspond to resting neutrophils labelled with

irrelevant antibodies, empty black curve correspond to neutrophils labelled with the 7D5 (anti-NOX2) or 449 antibodies ($p22^{phox}$) and secondary antibodies coupled with PE. (**f**) Genetic analysis of the mutation of patient P4a in *CYBB* gene, leading to an $X91^{-}$-CGD. NOX2 cDNA was amplified in 3 overlapping fragment as described in Materials and methods. A 124 bp of intron 3 was inserted between exon 3 and exon 4 leading to the creation of a pseudoexon. Intronic regions surrounding the inserted region of intron 3 in the NOX2 cDNA was amplified and sequenced. A c.253-1879A>G hemizygous mutation was found creating a splicing donor site, which unveils a cryptic acceptor site leading the inclusion of 124 nucleotides as a pseudo-exon responsible for the partial loss of the NOX2 expression. The consequence in the NOX2 protein is a missense mutation at Cys85 to Leu and a frameshift leading to the generation of a stop codon located 32 amino acids further on (p.Cys85LeufsX32).

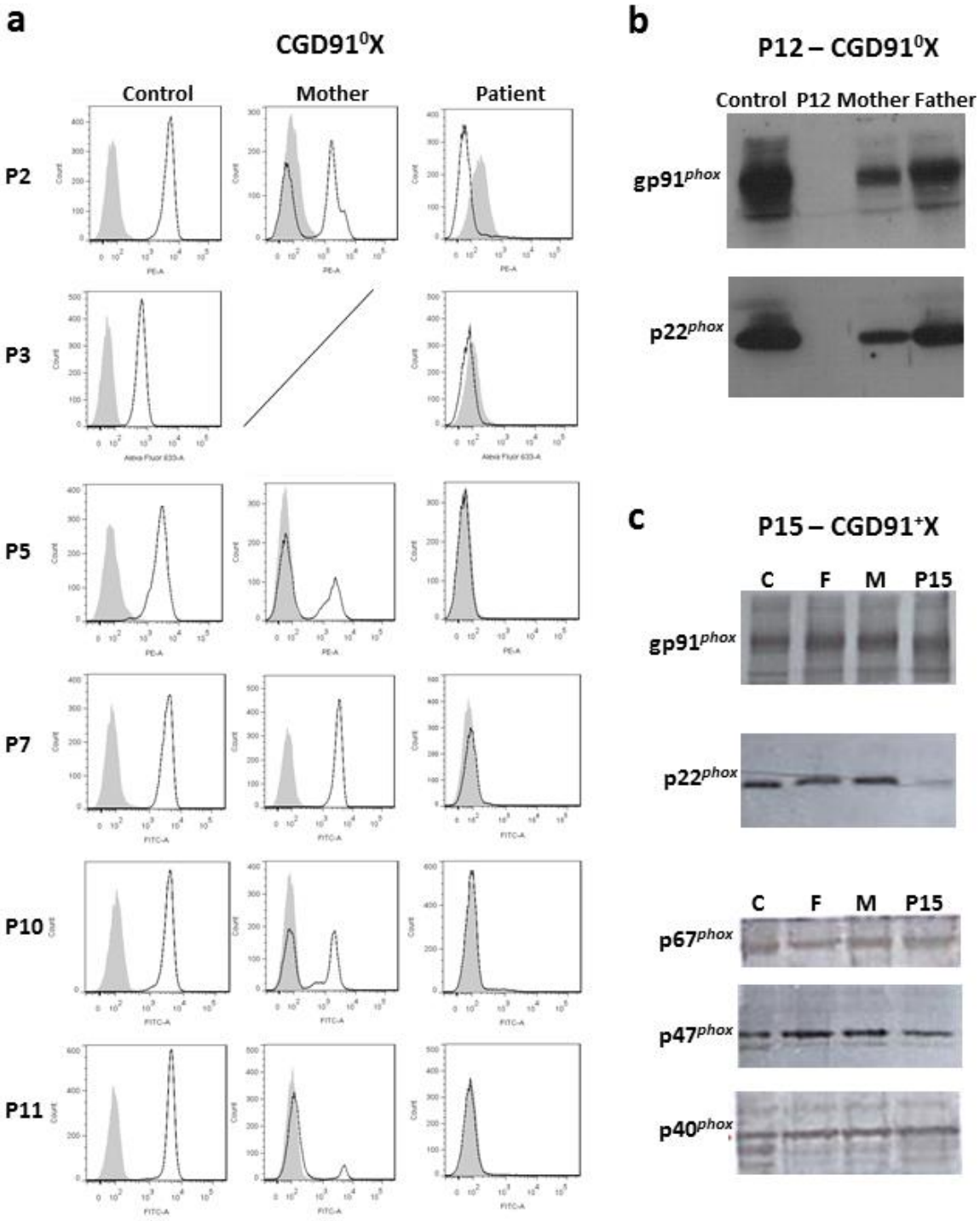
a
CGD91⁰X
Control
Mother
Patient
P2
P3
P5
P7
P10
P11
b
P12 – CGD91⁰X
Control P12 Mother Father
gp91phox
p22phox
c
P15 – CGD91⁺X
C F M P15
gp91phox
p22phox
C F M P15
p67phox
p47phox
p40phox

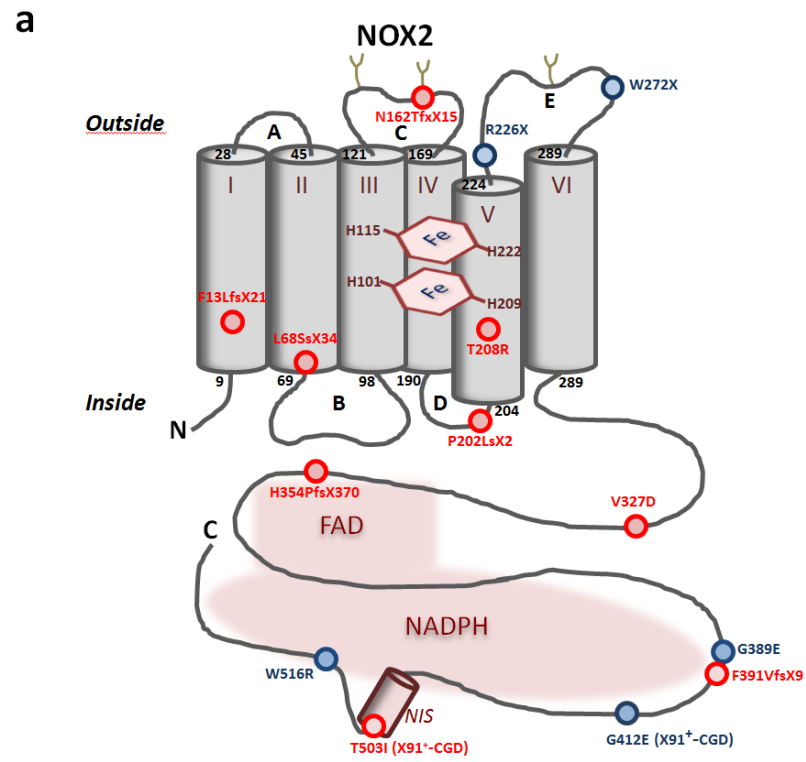
a
NOX2
Outside
Inside
N
C
A
B
C
D
E
I
II
III
IV
V
VI
28
45
121
169
224
289
9
69
98
190
204
289
H115
H222
H101
H209
Fe
Fe
N162TfxX15
R226X
W272X
F13LfsX21
L68SsX34
T208R
P202LsX2
H354PfsX370
V327D
FAD
NADPH
G389E
F391VfsX9
W516R
NIS
T503I (X91+-CGD)
G412E (X91+-CGD)

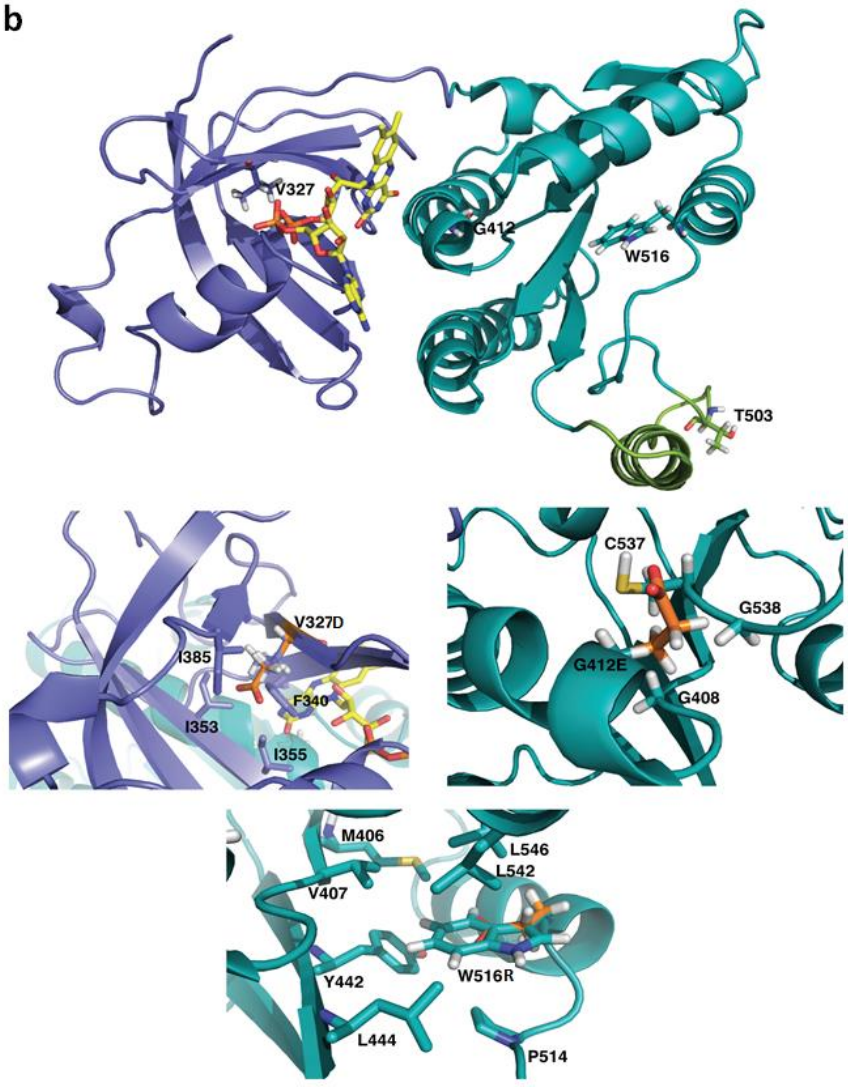
b
V327
G412
W516
T503
V327D
I385
F340
I353
I355
C537
G538
G412E
G408
M406
L546
L542
V407
Y442
W516R
L444
P514

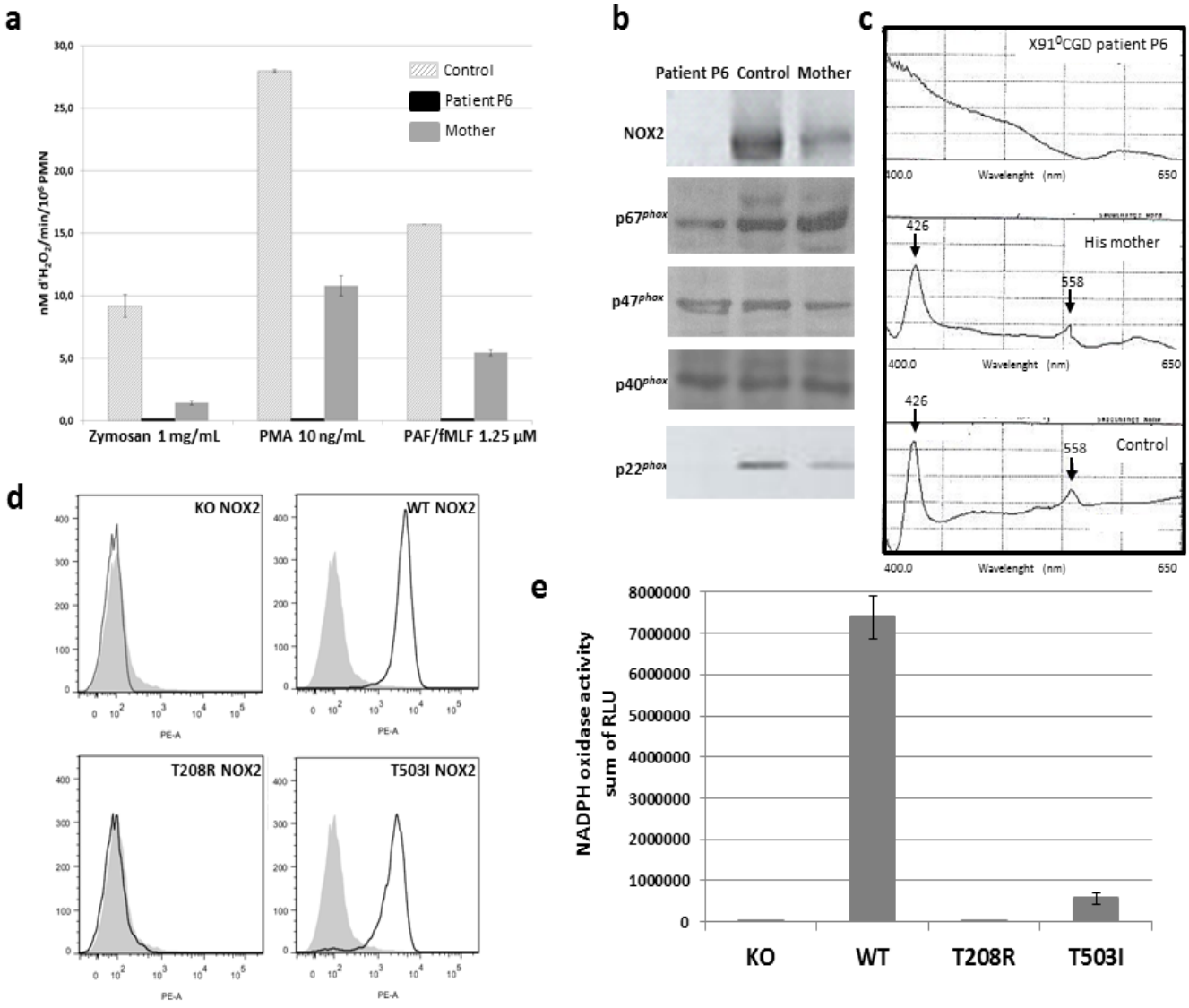
a
Control
Patient P6
Mother
Zymosan 1 mg/mL
PMA 10 ng/mL
PAF/fMLF 1.25 µM
b
Patient P6 Control Mother
NOX2
p67phox
p47phox
p40phox
p22phox
c
X91°CGD patient P6
His mother
Control
426
558
Wavelenght (nm)
d
KO NOX2
WT NOX2
T208R NOX2
T503I NOX2
PE-A
e
NADPH oxidase activity
sum of RLU
KO
WT
T208R
T503I

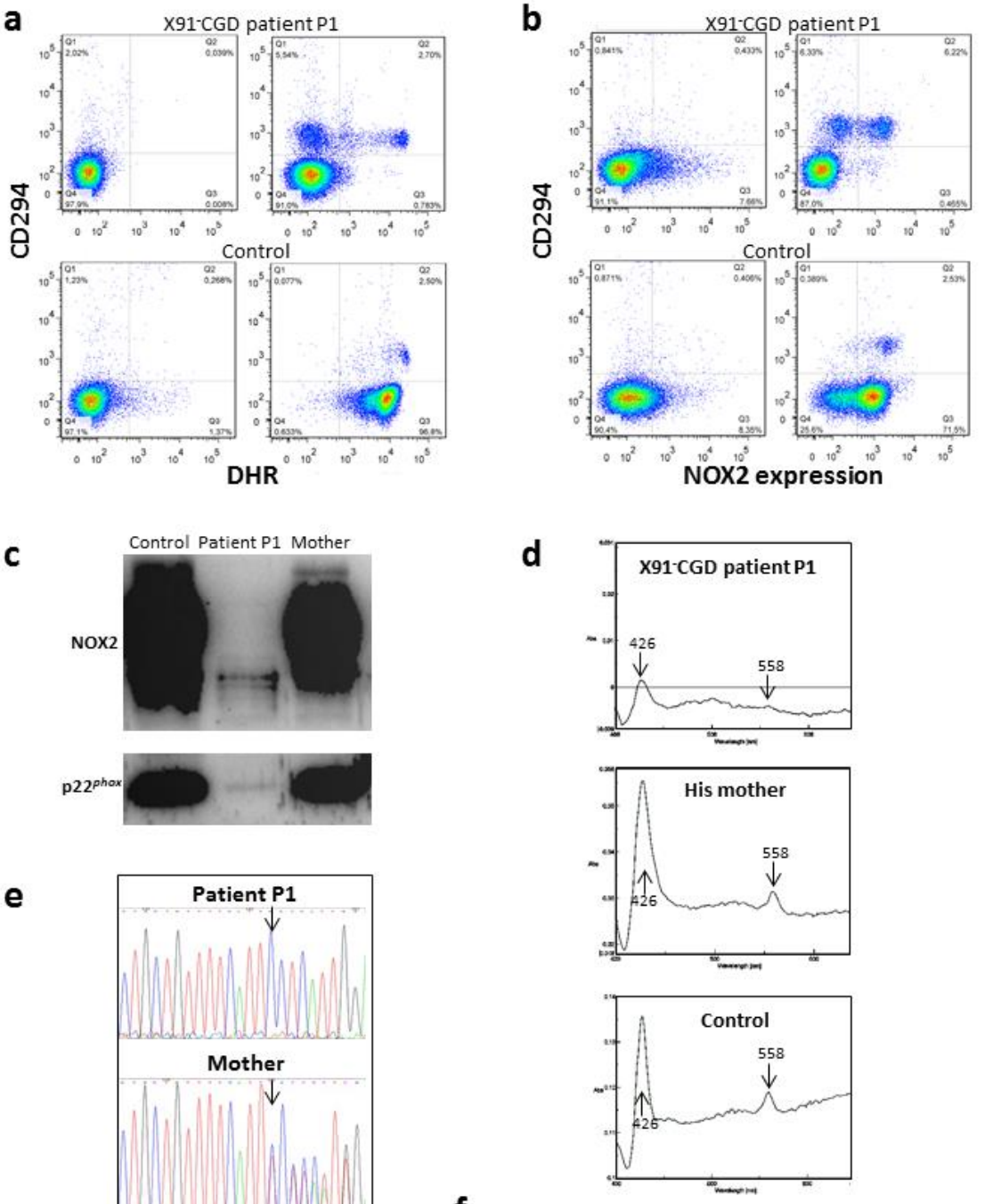
a
X91-CGD patient P1
CD294
Control
DHR
b
X91-CGD patient P1
CD294
Control
NOX2 expression
c
Control Patient P1 Mother
NOX2
p22phox
d
X91-CGD patient P1
426
558
His mother
558
426
Control
558
426
e
Patient P1
Mother
Control
f
cagttgaccaatgattattagccaatttctgataaaagaaa
aggaaaccgattgccccagggctgctgttttcaTT(T)cctc
-67delT
attggaagaagaagcatagtatagaagaaaggcaaacaca
acacattcaacctctgccacc ATG GGG...(exon 1)
-1 +1

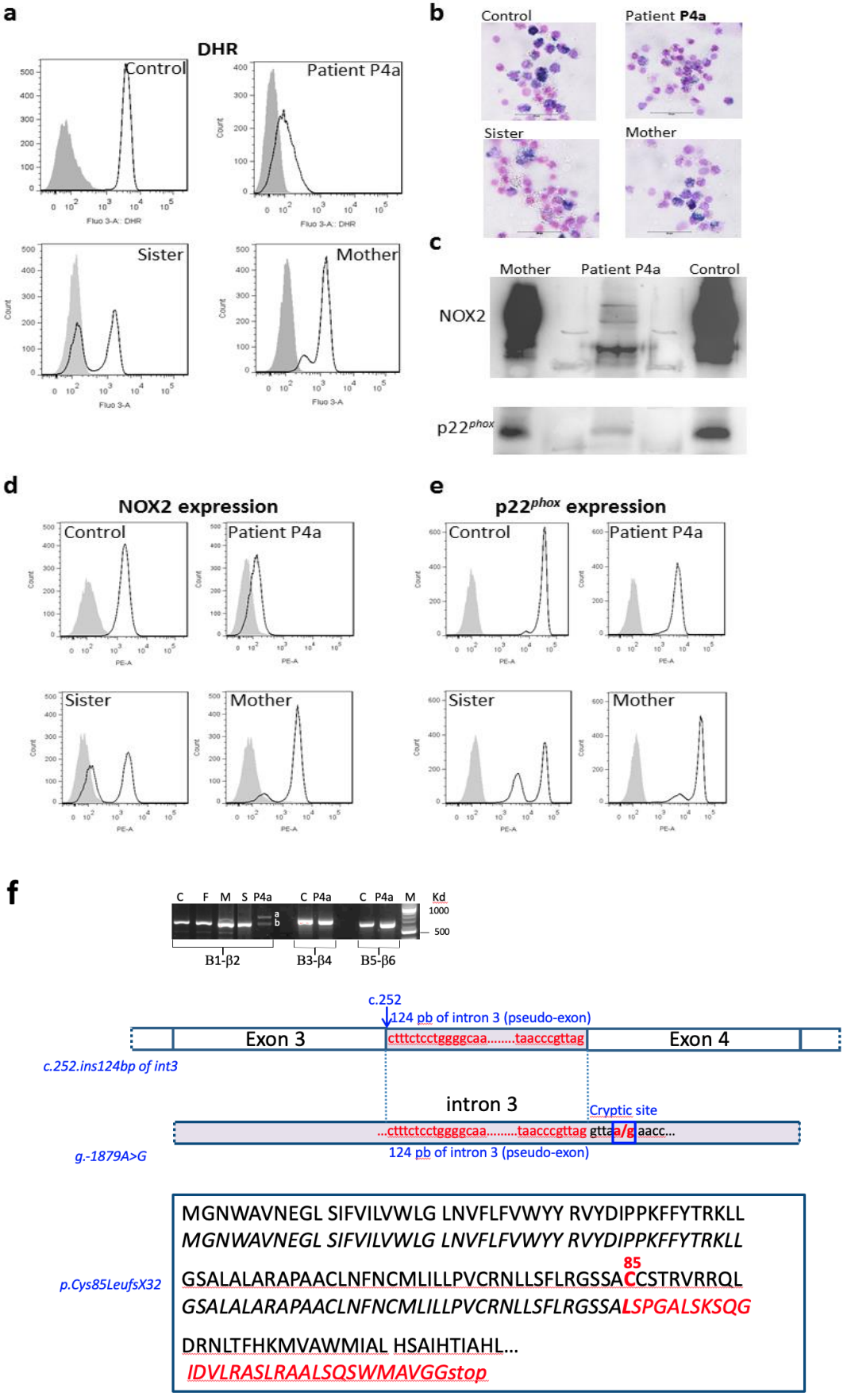
a
DHR
Control
Patient P4a
Sister
Mother
Fluo 3-A: DHR
Fluo 3-A
Count
b
Control
Patient P4a
Sister
Mother
c
Mother
Patient P4a
Control
NOX2
p22phox
d
NOX2 expression
Control
Patient P4a
Sister
Mother
PE-A
e
p22phox expression
Control
Patient P4a
Sister
Mother
PE-A
f
C F M S P4a C P4a C P4a M Kd
1000
500
a
b
B1-β2
B3-β4
B5-β6
c.252
124 pb of intron 3 (pseudo-exon)
Exon 3
ctttctcctggggcaa.....taacccgttag
Exon 4
c.252.ins124bp of int3
intron 3
Cryptic site
...ctttctcctggggcaa.....taacccgttag gttaa/g aacc...
g.-1879A>G
124 pb of intron 3 (pseudo-exon)
MGNWAVNEGL SIFVILVWLG LNVFLFVWYY RVYDIPPKFFYTRKLL
MGNWAVNEGL SIFVILVWLG LNVFLFVWYY RVYDIPPKFFYTRKLL
85
p.Cys85LeufsX32
GSALALARAPAACLNFNCMLILLPVCRNLLSFLRGSSACCSTRVRRQL
GSALALARAPAACLNFNCMLILLPVCRNLLSFLRGSSALSPGALSKSQG
DRNLTFHKMVAWMIAL HSAIHTIAHL...
IDVLRASLRAALSQSWMAVGGstop